Journal of Organometallic Chemistry, 390 (1990) C21–C26
Elsevier Sequoia S.A., Lausanne – Printed in The Netherlands
JOM 20963PC

Preliminary communication

Synthesis of organozinc enolates of *N,N*-disubstituted glycine esters. Crystal structure of [EtZnOC(OMe)=C(H)N(t-Bu)Me]$_4$

Fred H. van der Steen [a], Jaap Boersma [a], Anthony L. Spek [b] and Gerard van Koten [a]*

[a] *Debye Research Institute, Dept. of Metal-Mediated Synthesis, University of Utrecht, Padualaan 8, 3584 CH Utrecht (The Netherlands)*
[b] *Laboratory of Crystallography, University of Utrecht, Padualaan 8, 3584 CH Utrecht (The Netherlands)*

(Received January 27th, 1990)

Abstract

Pure ethylzinc α-amino ester enolates have been prepared from *N,N*-disubstituted glycine esters and *N*-(ethylzinc)diisopropylamine. An X-ray diffraction study of EtZnOC(OMe)=C(H)N(t-Bu)Me (**2b**) has shown it to be a tetrameric species, in which the four crystallographically independent zinc enolate units are interconnected via covalent Zn–O–Zn bridges. As a result of intramolecular Zn–N coordination, all the enolate moieties have the *Z*-configuration. ^{1}H NMR spectroscopy and molecular weight determinations in the case of **2b** indicate that in benzene the tetramer is in equilibrium with a dimeric species. In the dimer the Zn–N coordination is either weak, giving rise to a rapid on-off movement of the nitrogen, or totally absent.

The use of metal enolates in carbon–carbon coupling reactions has become an important tool in modern organic synthesis [1–3]. Most of the research in this field has involved alkali metal enolates [4,5], and very little is known about the structure and nature of metal enolates derived from less electropositive main-group metals, such as magnesium, aluminum, zinc, and tin.

Recently we reported that zinc enolates of *N,N*-disubstituted glycine esters, prepared in situ, reacted stereoselectively with imines to afford *trans*-3-amino-β-lactams, the principal building blocks of aztreonam and related monobactam antibiotics [6]. We believe that the high *trans*-stereoselectivity of these reactions is the result of a highly ordered transition-state involving the interaction of a *Z*-enolate with an *E*-imine. In order to seek support for this hypothesis and to gain further insight into the reaction mechanism, we have studied the structures of the intermediate zinc enolates in solution and in the solid state.

Zinc enolates of *N,N*-disubstituted glycine esters are easily prepared via transmetallation of the parent lithium enolates with a suitable zinc salt, e.g. $ZnCl_2$ or EtZnCl. However, elemental analyses of isolated zinc enolate prepared via this route, show the presence of tightly bound lithium chloride [6a]. In a recent paper by Hansen et al. it was shown that the zinc enolate of 2,2-dimethyl-3-pentanone can be formed by deprotonation with *N*-(ethylzinc)diisopropylamine (eq. 1), although the equilibrium constant for this reaction is close to unity [7].

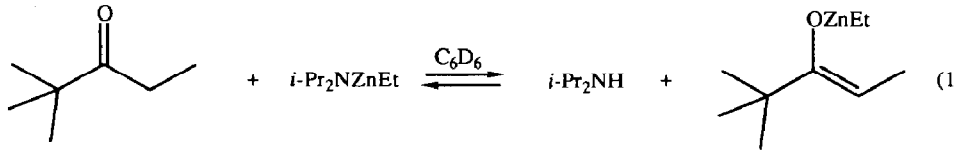

(1)

We have now prepared pure ethylzinc enolates (2)* of *N,N*-disubstituted glycine methyl esters (**1**) by direct deprotonation of **1** with *N*-(ethylzinc) diisopropylamine in benzene (eq. 2).

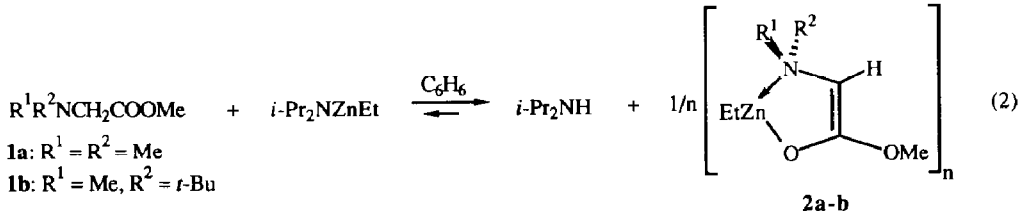

(2)

1a: $R^1 = R^2 = Me$
1b: $R^1 = Me$, $R^2 = t\text{-}Bu$

2a-b

After 24 h at room temperature all glycine ester has been deprotonated and the ethylzinc enolates **2a** and **2b** can be isolated (free of diisopropylamine) in nearly quantitative yields. It is very likely that these high yields are the result of the presence of the α-amino nitrogen which, through intramolecular coordination to zinc, will shift an equilibrium similar to that given in eq. 1 completely to the side of the product enolate.

It is noteworthy that these reactions of glycine esters **1a** and **1b** with *N*-(ethylzinc)diisopropylamine are far slower than those with LDA, which are complete within a few minutes.

Although the ^1H NMR spectra of **2a** ($R^1 = R^2 = Me$) show only broad resonances in the temperature range -70 to $80\,^\circ C$, the ^1H NMR spectra of **2b** (R^1 = t-Bu, R^2 = Me) show two distinct resonance patterns, the relative abundances of which are both temperature and concentration dependent **. However, the fact that these resonances show no coalescence or broadening between -70 and $80\,^\circ C$ indicates that there is a slow (on the NMR time-scale) interconversion between two species. Cryoscopic molecular weight measurements on **2b** in benzene indicate that this

* Physical data of EtZnOC(OMe)=C(H)N(t-Bu)Me (**2b**). ^1H NMR(tol-d_8; Me_4Si (ext.)): dimer; δ 4.02 (s, 1H, HC=C) 3.29 (s, 3H, OMe) 2.35 (s, 3H, NMe) 1.56 (t, J 8.0 Hz, 3H, CH_2CH_3) 1.11 (s, 9H, t-Bu) 0.55 (q, J 8.0 Hz, 2H, CH_2CH_3); tetramer; 3.83 (s, 1H, HC=C) 3.33 (s, 3H, OMe) 2.37 (s, 3H, NMe) 1.64 (t, J 8.1 Hz, 3H, CH_2CH_3) 1.20 (br.s, 9H, t-Bu) 0.76 (dq, J 8.1 and 13.1 Hz, $CH_aH_bCH_3$) 0.29 (dq, J 8.1 and 13.1 Hz, $CH_aH_bCH_3$). Anal. (calc.): C, 47.07 (47.54); H, 8.38 (8.41); N, 5.51 (5.54); Zn, 26.50 (25.88).

** At $-20\,^\circ C$ the dimer to tetramer ratio is ca. 1:4.5; at $50\,^\circ C$ this ratio is ca. 18:1 ([c] $\approx$ 0.30 *M*).

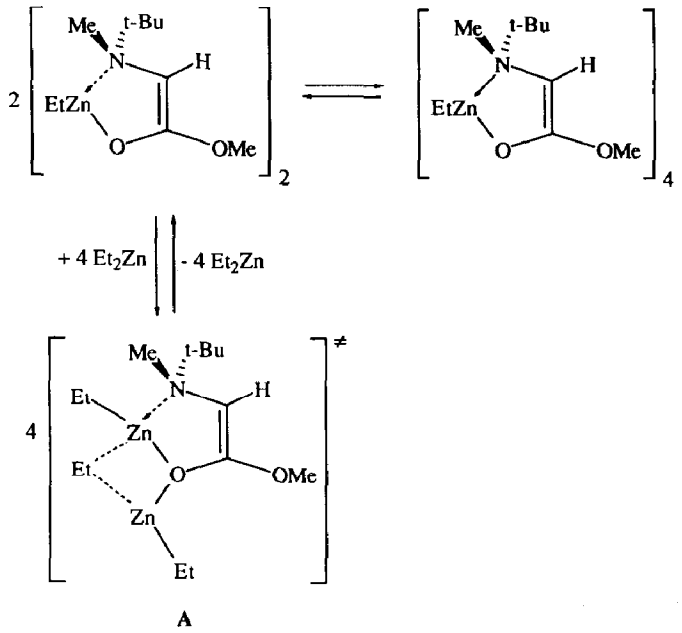

Scheme 1. The proposed equilibria for EtZnOC(OMe)=C(H)N(t-Bu)Me in benzene in the presence of Et_2Zn.

compound is present as a tetrameric species which is partly dissociated into dimers (Scheme 1). The degrees of association calculated from concentration-dependent cryoscopy agree well with the values obtained from concentration-dependent ^1H NMR spectroscopy, and this allows assignment of the individual resonance patterns to the tetramer or dimer.

The methylene protons of the Et-Zn moiety in the tetramer are diastereotopic and appear as an $AB(X)_3$ pattern with a large chemical shift difference of 0.47 ppm. This diastereotopicity indicates that zinc has become a stable chiral centre as a result of nitrogen-to-zinc coordination. In the dimer the methylene protons are not diastereotopic, and give rise to a single quartet. In this dimer therefore the Zn–N coordination is either weak, giving rise to a rapid on-off movement of the nitrogen, or is totally absent. This solution behaviour is in striking contrast to that of $[EtZnOC(Me)=C(H)N(t\text{-}Bu)Et]_2$ (3), a dimeric ethylzinc enolate with an intramolecularly coordinated β-amino nitrogen [8a]; the methylene protons of the Et–Zn moiety in this compound are diastereotopic between -70 and 80 °C [8b].

When diethylzinc is added to a solution of **2b** in toluene-d_8, ^1H NMR data show that the ethyl groups of the tetramer remain unchanged. In contrast, under these conditions the ethyl group bound to zinc in dimeric **2b** and those of diethylzinc become equivalent on the NMR time-scale. This means that there is a rapid exchange of ethyl groups between two (or more) zinc centres, probably via an intermediate dinuclear species **A** (Scheme 1). Noyori [9] has proposed a similar structure for the active intermediate in his enantioselective alkylations of aldehydes with dialkylzinc reagents that are catalyzed by chiral β-aminoalcohols.

The fact that the ethyl group bound to zinc in tetrameric **2b** does not exchange with those of added diethylzinc implies that diethylzinc does not have sufficient

Lewis acidity to break up the tetrameric unit. An important point is that the presence of diethylzinc does not noticably influence the dimer–tetramer equilibrium of **2b**, and we can therefore conclude that tetrameric **2b** is the most stable species in solution.

Unambiguous proof for a tetrameric structure of EtZnOC(OMe)=C(H)N(t-Bu)Me (**2b**) in the solid state comes from the X-ray structure determination *. The crystal structure of **2b** is monoclinic. The unit cell contains four tetrameric units, each of which contains four crystallographically independent enolate units. Although each tetrameric unit has approximate S_4 axial symmetry, this symmetry element does not coincide with a crystallographic axis. Figure 1 presents a view of the molecule and the numbering scheme used. Selected bond distances and angles are listed in Table 1.

The monomeric zinc enolate units of the tetramer are linked via covalent zinc–oxygen–zinc bridges (average Zn–O–Zn angle of 131.8°), which form a central, eight-membered Zn_4O_4 ring (puckering amplitude $Q = 2.561(3)$ Å [10]). The Zn–O bond lengths are normal (2.028(5) to 2.076(6) Å), but the somewhat larger differences in Zn–O bond lengths found in the Zn_2O_2 rings of $Ph_2Zn_3(acac)_4$ (**4**) (2.011(4) and 2.086(5) Å) [11] and of $[EtZnOC(Me)=C(H)N(t\text{-}Bu)Et]_2$ (**3**) (2.02(1) and 2.12(1) Å) [8a] are absent. The larger bond lengths in the latter structures correspond to dative Zn–O bonds. However, in **2b** the Zn–O bonds in each monomeric unit are longer than the (formally dative) Zn–O bonds between the monomeric units. While the Zn–O bonds in **3** and **4** are for the greater part ionic (with sp^3-hybridized bridging oxygen atoms), the Zn–O bonds in **2b** are more covalent, as is expressed by the Zn–O bond lengths and the sp^2-hybridized character of the trigonally surrounded bridging oxygen atoms.

In **2b** the intramolecular coordination of the amino nitrogen atoms to the zinc atoms results in the formation of essentially planar five-membered ZnOCCN chelate rings, which are orientated at angles ranging from 60.9(4)° to 77.9(4)° with respect to each other, to form an overall propeller-like structure. The central carbon–carbon bond lengths of the enolate **2b** (mean 1.327 Å) are significantly longer than the C=C double bond of 1.27(3) Å in dimeric **3**. This feature and the relatively short enolato carbon–oxygen bonds (mean 1.314 Å for the enolato (1.40(2) Å in **3**) and 1.364 Å for the methoxy oxygen) indicate that the electron

* *Crystal data*: $C_{40}H_{84}N_4O_8Zn_4$, $M = 1010.64$, monoclinic, $P2_1/n$, a 20.063(1), b 12.875(1), c 20.414(1) Å, $\beta = 101.72(1)°$, U 5163.2(6) Å^3, $Z = 4$, D_c 1.30 g cm^{-3}, $F(000) = 2144$, μ 19.3 cm^{-1} for Mo-K_α (0.71073 Å). A colourless crystal (0.35×0.25×0.15 mm) was sealed under nitrogen in a Lindemann glass-capillary and mounted on an Enraf-Nonius CAD4F diffractometer. Unit cell dimensions were calculated from the setting angles of 21 carefully centered reflections. 13018 unique data of one quadrant of the reflection sphere ($\pm h$, $+k$, $+l$) were collected in the $\omega/2\theta$ scan mode ($2.04 \leq 2\theta \leq 56.98°$), using Zr-filtered Mo-$K_\alpha$ radiation and corrected for Lorentz, polarization and absorption effects (DIFABS). The structure was solved by standard Patterson and Fourier methods (SHELXS-86) and refined on F by blocked full-matrix least-squares techniques (SHELX-76). Hydrogen atoms were introduced on calculated positions (C–H = 0.98 Å) and refined riding on their carrier atoms with two common isotropic thermal parameters, one for the CH_3 groups and one for the CH_2 and CH groups the final values being 0.103(7) and 0.061(13) Å^2, respectively. The refinement converged at $R = 0.061$ and $R_w = 0.055$ ($w = 1/\sigma^2(F)$) for 4114 reflections with $I > 2.5\ \sigma(I)$. A table of atomic coordinates and a complete list of bond lengths and angles has been deposited with the Cambridge Crystallographic Data Centre.

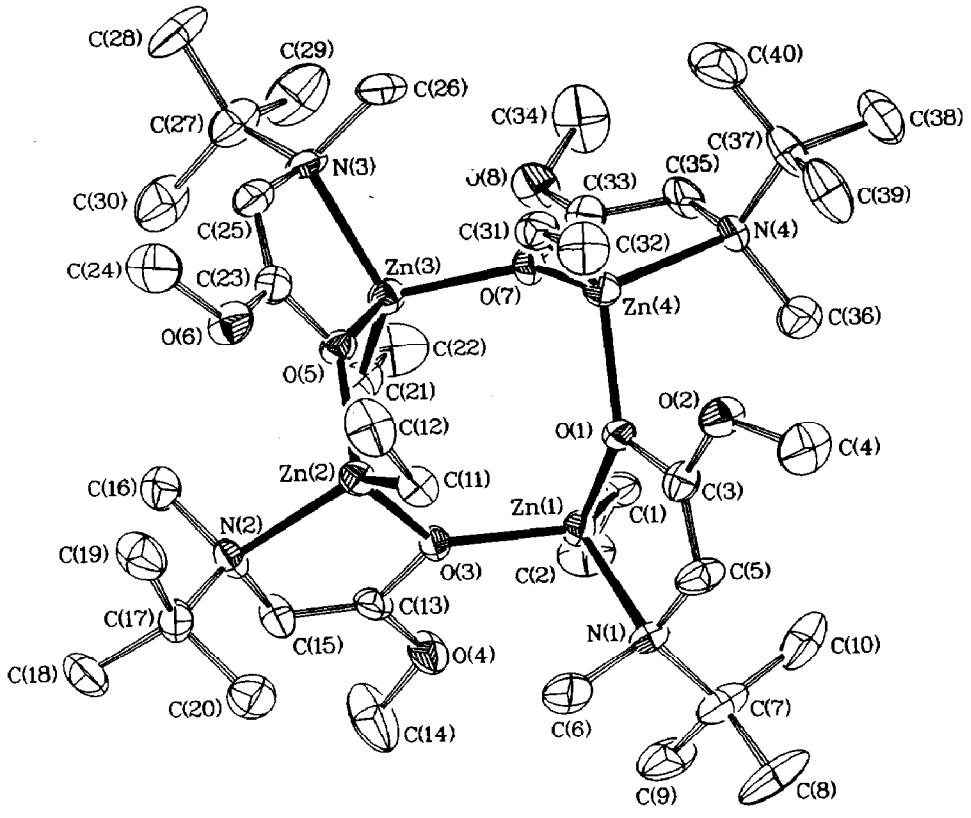

Fig. 1.

density in **2b** is partly delocalized, whereas in **3** there is no such delocalization. This could well be the reason that ester enolates **2**, which contain an electron-withdrawing methoxy substituent, show a different reactivity towards electrophiles (e.g. aldehydes and imines) than **3**, which contains a moderately electron-donating methyl substituent.

The zinc atoms in **2b** have a distorted tetrahedral coordination geometry, with three small (≈ 82, 95 and 100°) and three large angles (≈ 116, 123 and 129°), similar to that in **3**. The zinc–carbon distances (mean 1.978 Å) are in good agreement with those reported for **3**, $Et_2Zn_4[N(Ph)CO_2Me]_6$ [12a] and

Table 1

Selected bond lengths (Å) and angles (°) for **2b**, with esd's in parentheses [a]

Zn(1)–O(1)	2.061(6)	Zn(1)–O(3)	2.037(6)	Zn(1)–N(1)	2.206(8)
Zn(1)–C(1)	1.973(1)	Zn(2)–O(3)	2.056(6)	Zn(4)–O(1)	2.034(7)
O(1)–C(3)	1.325(12)	O(2)–C(3)	1.348(12)	O(2)–C(4)	1.410(12)
C(3)–C(5)	1.322(15)				
O(1)–Zn(1)–O(3)	95.3(2)	O(1)–Zn(1)–N(1)	82.1(3)		
O(1)–Zn(1)–C(1)	115.7(3)	O(3)–Zn(1)–N(1)	100.6(3)		
O(3)–Zn(1)–C(1)	122.1(3)	N(1)–Zn(1)–C(1)	129.7(4)		
Zn(1)–O(1)–Zn(4)	131.6(3)	Zn(1)–O(3)–Zn(2)	132.1(3)		

[a] The molecular structure consists of four independent enolate units with comparable geometry. For the sake of brevity the geometrical data of only one enolate unit are given.

$[EtZnOC(CH_2NEt_2)=Cp]_2$ [12b] (1.99(2), 1.963(5) and 1.957(3) Å, respectively). The zinc–nitrogen dative bond lengths (mean 2.211 Å) differ little from those of 2.21(2) Å for **3** and 2.19(3) Å for $Me_2N(CH_2)_3ZnW(Cp)(CO)_3$ [12c], but they are significantly larger than those in $[EtZnOC(CH_2NEt_2)=Cp]_2$ (2.121(2) Å). As a result of the intramolecular Zn–N coordination the configuration of the enolate in the solid state is, as expected, *Z*.

In solution at 50 °C this Zn–N coordination is very weak or even totally absent, so isomerization (via rotation about the central carbon–carbon bond) to an *E*-configuration cannot be ruled out. However, trapping experiments of the chlorozinc enolate (prepared in situ) with trimethyl silyl chloride show unambiguously that in this enolate the *Z*-configuration is maintained *.

Now that we have available the pure zinc enolates, we can study in more detail the mechanism of their reactions with imines (to afford β-lactams) and the influence of solvent and additives (lithium salts, amines) on the stereoselectivity of these reactions. The results of these studies will be reported in a forthcoming paper.

Acknowledgement. This research has been financially supported by Gist-Brocades N.V., The Netherlands and supported in part (A.L.S.) by the Netherlands Foundation for Chemical Research (SON) with financial aid from the Netherlands Organisation for Advancement of Pure Research (NWO).

References

1 see for example D.A. Evans, Stereoselective alkylation reactions of chiral metal enolates, in: J.D. Morrison (Ed.), Asymmetric Synthesis, Vol. 3, Academic Press, New York, 1983, pp. 1–110 and references cited therein.
2 C.H. Heathcock, The aldol addition reactions, in: J.D. Morrison (Ed.), Asymmetric Synthesis, Vol. 3, Academic Press, New York, 1983, pp. 111–212 and references cited therein.
3 D.A. Evans, J.V. Nelson and T.R. Taber, Stereoselective aldol condensations, in: N.J. Allinger, E.L. Eliel and S.H. Wilen (Eds.), Topics in Stereochemistry, Vol. 13, Wiley, New York, 1982.
4 L.M. Jackman and B.C. Lange, Tetrahedron, 33 (1977) 2737.
5 D. Seebach, Angew. Chem., 100 (1988) 1715.
6 (a) J.T.B.H. Jastrzebski, F.H. van der Steen, and G. van Koten, Recl. Trav. Chim. Pays-Bas, 106 (1987) 516; (b) F.H. van der Steen, J.T.B.H. Jastrzebski and G. van Koten, Tetrahedron Lett., 29 (1988) 2467; (c) F.H. van der Steen, H. Kleijn, J.T.B.H. Jastrzebski and G. van Koten, ibid., 30 (1989) 765; (d) idem, J. Chem. Soc., Chem. Commun., (1990) 503.
7 M.H. Hansen, P.A. Bartlett and C.H. Heathcock, Organometallics, 6 (1987) 2069.
8 (a) M.R.P. van Vliet, G. van Koten, P. Buysingh, J.T.B.H. Jastrzebski and A.L. Spek, Organometallics, 6 (1987) 537; (b) The ^1H and ^{13}C NMR data were collected by the current author (F.H.S.) in the range from −70 to 80 °C.
9 R. Noyori, Chem. Soc. Rev., 18 (1989) 187.
10 D. Cremer and J.A. Pople, J. Am. Chem. Soc., 97 (1975) 1354.
11 Spek, A.L., Cryst. Struct. Commun., 3 (1973) 535.
12 (a) F.A.J.J. van Santvoort, H. Krabbendam, A.L. Spek and J. Boersma, Inorg. Chem., 17 (1978) 388; (b) J.T.B.H. Jastrzebski, J. Boersma, G. van Koten, W.J.J. Smeets and A.L. Spek, Recl. Trav. Chim. Pays-Bas, 107 (1988) 263; (c) P.H.M. Budzelaar, H.J. Alberts-Jansen, K. Mollema, J. Boersma, G.J.M. van der Kerk, A.L. Spek and A.J.M. Duisenberg, J. Organomet. Chem., 243 (1983) 137.

* The *Z*-configuration of the formed silyl ketene acetal was confirmed by ^1H NOE-difference NMR spectroscopy.